Using Phonon Resonances as a Route to All-Angle Negative Refraction in the Far-Infrared Region: The Case of Crystal Quartz

R. Rodrigues da Silva,[1,*] R. Macêdo da Silva,[1] T. Dumelow,[1,†] J. A. P. da Costa,[1] S. B. Honorato,[2] and A. P. Ayala[2]

[1]*Departamento de Física, Universidade do Estado do Rio Grande do Norte, Costa e Silva, 59610-090 Mossoró RN, Brazil*
[2]*Departamento de Física, Universidade Federal do Ceará, Campus Pici, 60455-900 Fortaleza CE, Brazil*

We consider how all-angle negative refraction may be induced in anisotropic crystals by making use of the phonon response. We investigate the example of crystal quartz at far-infrared wavelengths. Reflection and transmission measurements confirm the expected behavior, and show relatively high transmission efficiency at frequencies at which negative refraction occurs.

PACS numbers: 42.25.Bs, 42.25.Lc, 71.36.+c

Among the various ways used to obtain negative refraction, possibly the simplest is to make use of nonmagnetic anisotropic materials. We consider a beam to undergo negative refraction if, on passing through an interface from air to such a material, the incident and refracted rays lie on the same side of the surface normal. We stress that, in this Letter, our principal interest is in ray direction (as opposed to wave-vector direction), corresponding to the direction of power flow, and we are defining negative refraction accordingly. In this sense, negative refraction of the extraordinary ray in any anisotropic crystal is possible if one of its principal axes makes an oblique angle with the surface normal, as observed in crystals such as calcite at visible frequencies [1]. Nevertheless, the range of incident angles over which this occurs is generally very narrow. Of considerably more interest, in the context of recent studies, is negative refraction for all incident angles, both positive and negative, a phenomenon traditionally associated with artificial metamaterial or photonic band-gap structures [2,3], but also exhibited by certain metallic ferromagnets at gigahertz frequencies [4]. A material which leads to this type of negative refraction can, in principle, be used in planar slab lens structures [5,6].

All-angle negative refraction of the type described above may occur in a nonmagnetic anisotropic material if two of its principal components have opposing signs [7–11]. The majority of studies of negative refraction based on this principle consider an artificial metamaterial, such as a superlattice [7,11–13] or metallic nanowire [14] structure, as the anisotropic material. In the mid- to far-infrared range, most work has concentrated on semiconductor superlattices, making use of either the phonon response [7,11] or the plasmon response in doped samples [15] to achieve the correct form of the dielectric tensor. In the latter case, convincing experimental evidence of negative refraction has been demonstrated. Despite the success achieved using artificial structures, it should not be forgotten that, over a limited frequency range, many natural anisotropic crystals exhibit a dielectric tensor having the required form [9,10,16]. Indeed, it has been predicted that,

at low temperatures, all-angle negative refraction may be possible in certain crystals with negligible absorption in the far-infrared region [9]. In this Letter we investigate room temperature negative refraction based on the phonon response in anisotropic crystals, using crystal quartz as our example. In this case, absorption plays a vital role, and we show, both theoretically and experimentally, its effect on a negatively refracting beam as it passes through a quartz crystal. Crystals for the study were bought commercially from Boston Piezo-Optics, and spectroscopic measurements were made using a Bruker Vertex 70 spectrometer.

The geometry used in the present study may be represented as shown in Fig. 1. We consider *p*-polarized incident radiation (**E** field in the plane of incidence *xz*) obliquely incident from air onto the anisotropic medium. This medium is uniaxial, with its uniaxis normal to the sample surface, along *z*.

For angle of incidence θ_1, the in-plane wave-vector component k_x is then given by $k_x = k_0 \sin\theta_1$, where $k_0 = \omega/c$. Boundary conditions dictate that this k_x value holds both sides of the interface. The *z* component of the wave vector in air is simply given by $k_{1z}^2 = k_0^2 - k_x^2$, but within the crystal it is given by

$$k_{2z}^2 = k_0^2 \epsilon_{xx} - k_x^2 \frac{\epsilon_{xx}}{\epsilon_{zz}}, \qquad (1)$$

where ϵ_{xx} and ϵ_{zz} represent the principal components of the dielectric function of the uniaxial medium. The correct
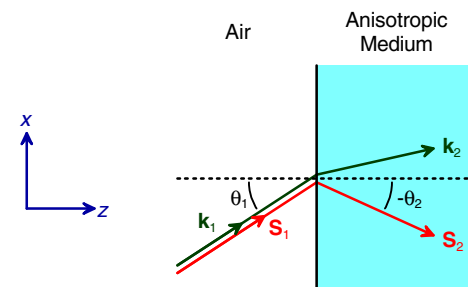
FIG. 1 (color online). Geometry considered in this Letter showing wave vector and Poynting vector directions.

sign of k_{2z} is determined by the condition that power flow must be away from the interface [7] (or, if the field is purely evanescent, decay must be away from the interface).

The angle of refraction θ_2 is most usefully expressed as the direction of the power flow in the anisotropic medium. This can be determined from the Poynting vector $\mathbf{S}_2$, whose time-averaged value is given by $\langle \mathbf{S}_2 \rangle = \frac{1}{2} \mathrm{Re}(\mathbf{E} \times \mathbf{H}^*)$. θ_2 is then given by [9]

$$\tan\theta_2 = \frac{\langle S_{2x} \rangle}{\langle S_{2z} \rangle} = \frac{\mathrm{Re}(k_x / \epsilon_{zz})}{\mathrm{Re}(k_{2z} / \epsilon_{xx})}. \quad (2)$$

In order to gain a physical insight of how negative refraction can arise due to the presence of anisotropy, we can ignore damping as a first approximation. In this case ϵ_{xx} and ϵ_{zz} are both real, and k_{2z} can be either real or imaginary (the necessary conditions for each of these cases are summarized in [7,8]). When k_{2z} is imaginary, all the incident radiation is reflected, and $\theta_2 = \pm 90°$, corresponding to an evanescent wave propagating along the surface. When k_{2z} is real, however, radiation propagates into the sample, and $|\theta_2| < 90^0$. Of particular interest is the case when $\epsilon_{xx} > 0$, $\epsilon_{zz} < 0$, in which case k_{2z} is both real and positive. Since k_x and θ_1 both have the same sign, θ_1 and θ_2 now have opposing signs, i.e., negative refraction should occur.

Effective medium theory shows that the condition $\epsilon_{xx} > 0$, $\epsilon_{zz} < 0$ may be obtained by constructing super-lattice structures [17], and this principle has been the basis of several mid- to far-infrared studies [7,11,15]. Our approach in this Letter, however, is to make use of the phonon response in natural uniaxial crystals. The dielectric function associated with the phonon response in such crystals at frequency ω may be written in the form

$$\epsilon_{uu} = \epsilon_{\infty,u} \prod_n \frac{\omega_{\mathrm{L}n,u}^2 - \omega^2 - i\omega\gamma_{\mathrm{L}n,u}}{\omega_{\mathrm{T}n,u}^2 - \omega^2 - i\omega\gamma_{\mathrm{T}n,u}}, \quad (3)$$

where u represents either x or z, $\epsilon_{\infty,u}$ is the high frequency dielectric constant, $\omega_{\mathrm{T}n,u}$ and $\omega_{\mathrm{L}n,u}$ are the frequencies of transverse optical (TO) and longitudinal optical (LO) phonon modes, respectively, and $\gamma_{\mathrm{T}n,u}$ and $\gamma_{\mathrm{L}n,u}$ are their respective damping parameters. In the zero absorption approximation, we simply put $\gamma_{\mathrm{L}n,u} = \gamma_{\mathrm{L}n,u} = 0$ for all n. In general, whenever ω lies between $\omega_{\mathrm{T}n,u}$ and the corresponding $\omega_{\mathrm{L}n,u}$ value, ϵ_{uu} is negative. Since the phonon frequencies corresponding to polarization along x may be different from those corresponding to polarization along z, it may be possible to satisfy the condition $\epsilon_{xx} > 0$, $\epsilon_{zz} < 0$ close to these frequencies.

Figure 2(a) shows the relevant tensor components, calculated using the experimental parameters of Gervais and Piriou [18], in the case of crystal quartz in the frequency range from 400 to 600 cm^{-1} [19]. The crystal's uniaxis is taken to be along z, and damping is ignored. In this axis system, poles and zeros in ϵ_{xx} occur at the E symmetry TO and LO phonon frequencies, respectively, whereas poles
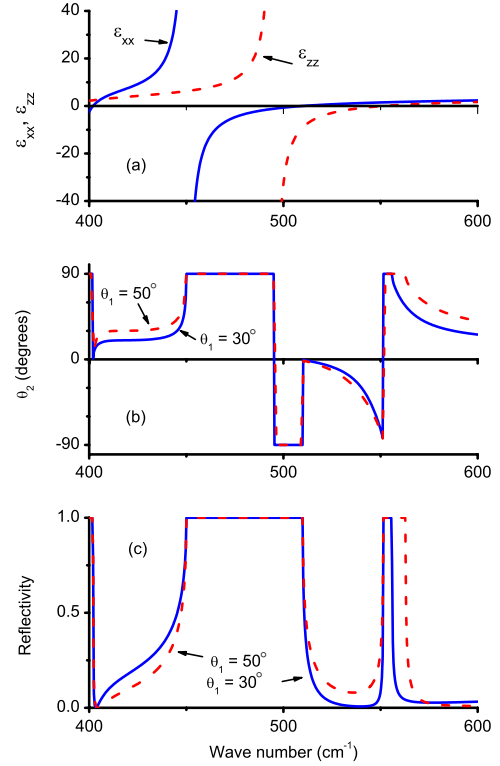
FIG. 2 (color online). Simulations for quartz, with uniaxis along z, in the absence of damping. (a) Dielectric tensor components ϵ_{xx} and ϵ_{zz}; (b) p-polarized angle of refraction from air; (c) p-polarized reflectivity. In (b) and (c) the solid and dashed lines represent incident angles of 30° and 60°, respectively.

and zeros in ϵ_{zz} occur at the corresponding A_2 symmetry phonon frequencies. It can be seen that, in the frequency range shown, there are various combinations of signs of ϵ_{xx} and ϵ_{zz}. In particular, the condition $\epsilon_{xx} > 0$, $\epsilon_{zz} < 0$ is satisfied in the range 510 to 551 cm^{-1} (i.e., between the E and A_2 symmetry LO phonon frequencies), so negative refraction should be possible in this region. This is confirmed in Fig. 2(b), which shows the calculated p-polarization angles of refraction for incident angles of 30° and 50°. The negative refraction region is bounded by two total reflection regions with k_{2z} imaginary and $\theta_2 = \pm 90°$. That reflection is total in these two regions, but finite in the negatively refracting region (510 to 551 cm^{-1}) is confirmed in Fig. 2(c), which shows the simulated reflectivity spectra for the same angles of incidence. It is noticeable that reflectivity is very low in the negatively refracting region, suggesting that transmission into the crystal should be efficient in this frequency range.

Clearly the presence of absorption is, in practice, an important consideration. In this case the dielectric tensor components become complex, as does k_{2z}. We can now, to a good approximation, replace the negative refraction requirement $\epsilon_{xx} > 0$, $\epsilon_{zz} < 0$ by $\mathrm{Re}(\epsilon_{xx}) > 0$, $\mathrm{Re}(\epsilon_{zz}) < 0$. This can be seen by comparing Figs. 3(a) and 3(b) which show, respectively, the real parts of the dielectric tensor
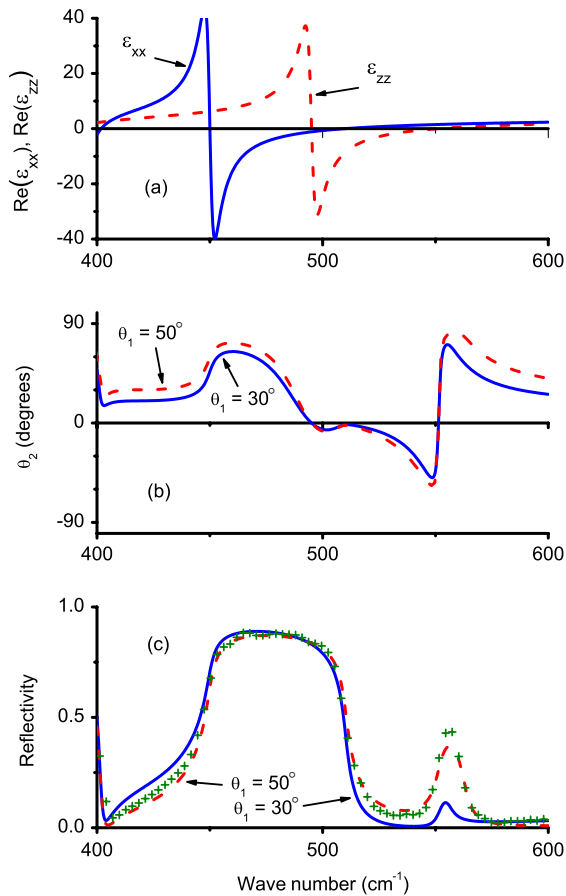
FIG. 3 (color online). Simulations for quartz, with uniaxis along z, using published damping parameters, along with experimental reflectivity. (a) Real part of the dielectric tensor components ϵ_{xx} and ϵ_{zz}; (b) p-polarized angle of refraction from air; (c) p-polarized reflectivity. In (b) and (c) the solid and dashed lines represent incident angles of incidence of 30° and 60°, respectively. The crosses in (c) represent experimental results.

components and the angles of refraction when published damping parameters [18] are incorporated into the modeled dielectric function [Eq. (3)].

The frequency region 510 to 551 cm^{-1} is confirmed to be a region of negative refraction, as before. We can also see from the reflectivity results in Fig. 3(c) that this region is once again bounded by two high reflectivity regions, although reflection is no longer total. The additional experimental measurements, obtained using a diffuse reflection accessory with an average incident angle of about 50°, are in good agreement with theory for $\theta_1 = 50°$, giving further support to our predictions.

So far we have considered phonon damping in terms of its effect on reflection and angle of refraction. However, for negative refraction to be useful, transmission through a crystal should occur with a minimum of absorption, so it is also important to study the transmission behavior.

In Fig. 4 we show theoretical and experimental p-polarized spectra for transmission through a freestanding
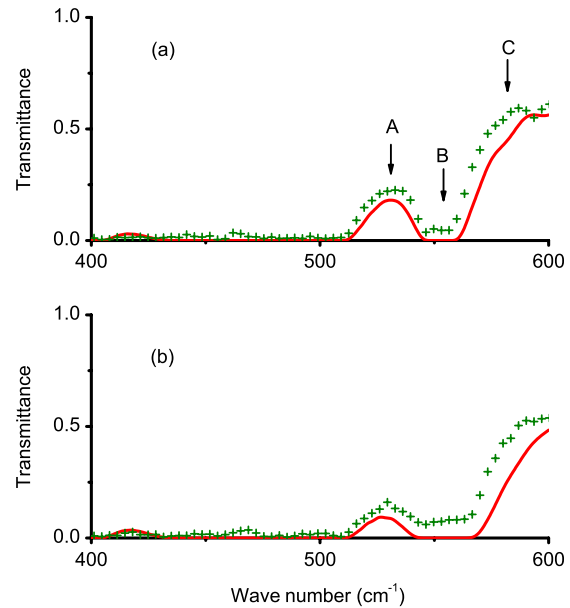
FIG. 4 (color online). Theoretical (solid lines) and experimental (crosses) p-polarized transmission spectra through a 50 μm thick quartz crystal for angles of incidence (a) 30° and (b) 50°.

50 μm thick z-cut quartz crystal, for incident angles of 30° and 50°. In general, there is good agreement between theory and experiment, although, due to poor polarizer efficiency, there is some leakage of s-polarized radiation in the experimental measurements, leading, in practice, to a slightly higher transmission than theory predicts. Concentrating on the frequencies above 510 cm^{-1}, we see that there is significant transmission within the region 510 to 551 cm^{-1}, where negative refraction is expected. The region around the A_2 symmetry LO phonon at 551 cm^{-1} is effectively opaque, and there is a further transmission region at higher frequencies.

The behavior in these three regions can be understood by considering the representative frequencies marked as A, B and C in Fig. 4(a). A simulation of a p-polarized Gaussian beam, modeled as a Fourier sum of plane waves [9], transmitted through a 50 μm thick quartz crystal at these three frequencies is shown in Fig. 5. The incident beam is focused onto the crystal surface at $x = 0$, $y = 0$.

At frequency A [Fig. 5(a)], we can see that the transmitted beam is displaced in the negative x direction with respect to the incident beam, thus demonstrating negative refraction. There is attenuation of the beam due to absorption, but transmission is still appreciable. Reflection is negligible, as expected from Fig. 3(c).

At frequency B [Fig. 5(b)], there is effectively no transmission through the crystal. Some of the radiation is reflected, as anticipated from Fig. 3(c), but more important is the high degree of absorption at this frequency. This is similar to the effect seen by Berreman [21], who reported LO phonon frequency dips in the p-polarized transmission spectra through thin isotropic films.
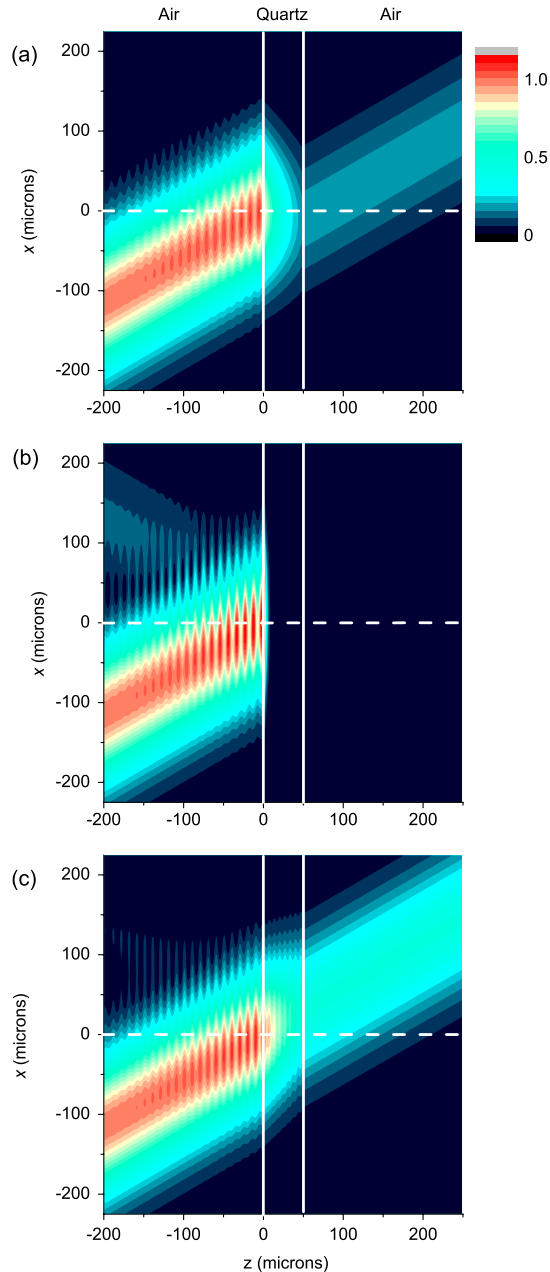
FIG. 5 (color online).   Simulation of the intensity profile of a
p-polarized Gaussian beam of width 100 μm passing through a
50 μm thick quartz crystal at an incident angle of 30° and
frequency (a)   531 cm^{-1} (frequency A),   (b)   554 cm^{-1}
(frequency B), and (b) 582 cm^{-1} (frequency C). The vertical
lines mark the two surfaces of the crystal, while the horizontal
dashed line shows the z axis at $x = 0$.

Frequency C [Fig. 5(c)] shows a positive displacement
of the transmitted beam, corresponding to positive refrac-
tion, as expected from Fig. 3(b). Transmission is somewhat
greater than in the negative refraction region, in agreement
with Fig. 4(a).

The above results show good agreement between experi-
ment and the various aspects of the theory. There is thus

convincing evidence of negative refraction in the fre-
quency range 510 to 551 cm^{-1}. It is also seen that,
although absorption is present, there is still significant
transmission in this region. A good quantitative measure
of the effect of absorption may be obtained from the
attenuation constant α [$= 2\,\mathrm{Im}(k_{2z})$]. For an angle of
incidence of 30° at frequency A, the absorption coefficient
is 330 cm^{-1}. For an angle of incidence of 50°, it is
450 cm^{-1}. These values are significantly better than those
obtained using semiconductor superlattices [15], even tak-
ing into account wavelength differences.

In summary, this study indicates that, although they lack
tunability, natural crystals show distinct promise as nega-
tively refracting media.

*Present address: Departamento de Física, UFRN, 59072-
970 Natal RN, Brazil.
†Corresponding author.
tdumelow@yahoo.com.br
[1] A. Boardman, N. King, and L. Velasco, Electromagnetics
25, 365 (2005).
[2] S. A. Ramakrishna, Rep. Prog. Phys. **68**, 449 (2005).
[3] C. Luo, S. G. Johnson, J. D. Joannopoulos, and J. B.
Pendry, Phys. Rev. B **65**, 201104(R) (2002).
[4] A. Pimenov, A. Loidl, K. Gehrke, V. Moshnyaga, and K.
Samwer, Phys. Rev. Lett. **98**, 197401 (2007).
[5] V. G. Veselago, Sov. Phys. Usp. **10**, 509 (1968).
[6] J. B. Pendry, Phys. Rev. Lett. **85**, 3966 (2000).
[7] T. Dumelow and D. R. Tilley, J. Opt. Soc. Am. A **10**, 633
(1993).
[8] P. A. Belov, Microw. Opt. Technol. Lett. **37**, 259 (2003).
[9] T. Dumelow, J. A. P. da Costa, and V. N. Freire, Phys. Rev.
B **72**, 235115 (2005).
[10] V. Dvorak and P. Kuzel, Ferroelectrics **338**, 195 (2006).
[11] L. V. Alekseyev and E. Narimanov, Opt. Express **14**,
11 184 (2006).
[12] M. Scalora *et al.*, Opt. Express **15**, 508 (2007).
[13] L. Shi and L. Gao, Phys. Rev. B **77**, 195121 (2008).
[14] Y. Liu, G. Bartal, and X. Zhang, Opt. Express **16**, 15 439
(2008).
[15] A. J. Hoffman *et al.*, Nature Mater. **6**, 946 (2007).
[16] V. A. Podolskiy, L. V. Alekseyev, and E. E. Narimanov, J.
Mod. Opt. **52**, 2343 (2005).
[17] N. Raj and D. R. Tilley, Solid State Commun. **55**, 373
(1985).
[18] F. Gervais and B. Piriou, Phys. Rev. B **11**, 3944
(1975).
[19] In their fit to experimental data, Gervais and Piriou include
a weak A_2 symmetry mode at 509 cm^{-1}. This is generally
considered to be an experimental artifact [18,20], and has
not been included in our simulations.
[20] J. L. Duarte, J. A. Sanjurjo, and R. S. Katiyar, Phys. Rev. B
36, 3368 (1987).
[21] D. W. Berreman, Phys. Rev. **130**, 2193 (1963).